POLITECNICO DI TORINO
Repository ISTITUZIONALE

Land use carbon emissions in China's coal-resource-based cities: Quantitative measurement and drivers analysis

Original
Land use carbon emissions in China's coal-resource-based cities: Quantitative measurement and drivers analysis / Pan, Y., Yang, X., Chen, L., Liu, L., Wang, C.. - In: URBAN CLIMATE. - ISSN 2212-0955. - 64:(2025). [10.1016/j.uclim.2025.102638]

Availability:
This version is available at: 11583/3007360 since: 2026-02-05T04:23:07Z

Publisher:
Elsevier

Published
DOI:10.1016/j.uclim.2025.102638

Terms of use:

This article is made available under terms and conditions as specified in the corresponding bibliographic description in the repository

Publisher copyright
Elsevier postprint/Author's Accepted Manuscript

© 2025. This manuscript version is made available under the CC-BY-NC-ND 4.0 license http://creativecommons.org/licenses/by-nc-nd/4.0/.The final authenticated version is available online at: http://dx.doi.org/10.1016/j.uclim.2025.102638

(Article begins on next page)

10 November 2026

Land Use Carbon Emissions in China's Coal-Resource-Based Cities: Quantitative Measurement and Drivers Analysis

Yisha Pan[1], Xiaoyan Yang [2], Longgao Chen[1], Liangchen Liu [1], Chongyang Wang [3]

1. College of Public Policy and Management (College of Emergency Management), China University of Mining and Technology, Xuzhou 221116;

2. College of Geography, Geomatics and Planning, Jiangsu Normal University, Xuzhou 221116;

3. School of Resources and Safety Engineering, Chongqing University, Chongqing, China, 400044.

** Correspondence: chenlonggao@163.com.*

Abstract: This study constructs a land use carbon emissions (LUCE) accounting framework based on panel data from China's coal-resource-based cities during 2000-2020. Through the integrated application of multiple linear regression, gravity center models, and spatial analysis techniques, it systematically reveals the driving mechanisms and spatiotemporal evolution patterns of LUCE. Key findings include: (1) Temporal analysis shows approximately 80% of cities exhibited a post-peak decline trend in LUCE between 2008-2018, with regenerative cities demonstrating the latest peaking timing and highest cumulative emissions, while declining cities maintained the lowest carbon emission intensity per unit GDP; (2) Mechanistic investigations identify distinct drivers across urban typologies: growing cities display significant sensitivity to topographic constraints and proximity to provincial capitals, mature cities are positively driven by climatic factors and mining industry scale, declining cities exhibit strong positive correlations with industrial structure rigidity and construction land expansion, whereas regenerative cities achieve emission suppression through human capital optimization and service-oriented industrial upgrading; (3) Spatial evolution patterns reveal a northeast-southwest axial migration of LUCE hotspots, transitioning from traditional industrial clusters in Liaoning-Hebei regions to central China's core zones (Henan), with sustained comprehensive low-emission equilibrium observed in southwestern China. These findings provide scientific support for implementing categorized and phased carbon reduction strategies in coal-resource-based cities.

Keywords: Coal Resource Cities; Land Use Carbon Emissions; Influencing Factors Analysis; Multiple Linear Regression

1 Introduction

Anthropogenically driven carbon emissions have significantly exacerbated global climate change, with land use transitions exerting particularly pronounced perturbation effects on regional

carbon cycles (Tao et al., 2025). Investigating the carbon effects of land use is critical for optimizing urban spatial structures and advancing low-carbon development. As pivotal components of China's energy-economic system, coal-resource-based cities (CRBCs) are characterized by their high energy consumption and carbon-intensive nature, positioning them as strategic focal points for achieving national carbon neutrality goals (Gu et al., 2023). In 2020, China integrated territorial spatial restructuring into its core pathway for green transition under the Dual Carbon Goals (carbon peaking by 2030 and carbon neutrality by 2060) (Mi et al., 2019; Guevara et al., 2020; Liu et al., 2015; Guan et al., 2021). Against this backdrop, systematically elucidating the spatiotemporal differentiation patterns and driving mechanisms of carbon emissions in CRBCs, as well as evaluating the dynamic impacts of land use changes on carbon sources/sinks, represents not only a scientific imperative for climate mitigation but also a crucial breakthrough in addressing the transformation challenges of resource-dependent cities (Zhang et al., 2018; Zhu et al., 2025).

Studies reveal that coal-resource-based cities (CRBCs) typically exhibit high carbon emission intensity and sluggish decoupling progress due to structural rigidities in industrial composition, entrenched energy consumption patterns, and lagging spatial planning (Chen et al., 2022; Guan et al., 2021). Their land use models are deeply intertwined with resource extraction activities, resulting in spatially clustered carbon emissions patterns (Bao et al., 2023; Christian et al., 2025). While existing research has explored land use carbon effects across multiple scales—encompassing carbon accounting models (Zhang et al., 2025), spatiotemporal heterogeneity in low-carbon land use (Zeng et al., 2025), emission drivers (Wu et al., 2022), and policy simulations (Paolo et al., 2024)—critical limitations persist: (1) a predominance of macro-scale analyses lacking systematic deconstruction of deep-seated mechanisms such as industrial structure lock-in effects and resource-dependent pathways in CRBCs (Hu et al., 2024); (2) policy simulations predominantly based on static assumptions, inadequately capturing the long-term impacts of multi-factor interactions on land use-related emissions (Cao et al., 2025; He et al., 2025; Feng et al., 2023; Xu et al., 2024; Zhang et al., 2024).

To address these gaps, this study focuses on CRBCs with the objectives of elucidating the spatiotemporal differentiation patterns of land use carbon emissions; uncovering the driving mechanisms of carbon emissions across developmental stages; and evaluating the dynamic impacts of land use changes on carbon sources/sinks, thereby providing theoretical guidance and scientific support for achieving the Dual Carbon Goals.

2. Study Area and Methodology

2.1 Study Area Overview and Data Sources

2.1.1 Study Area Description

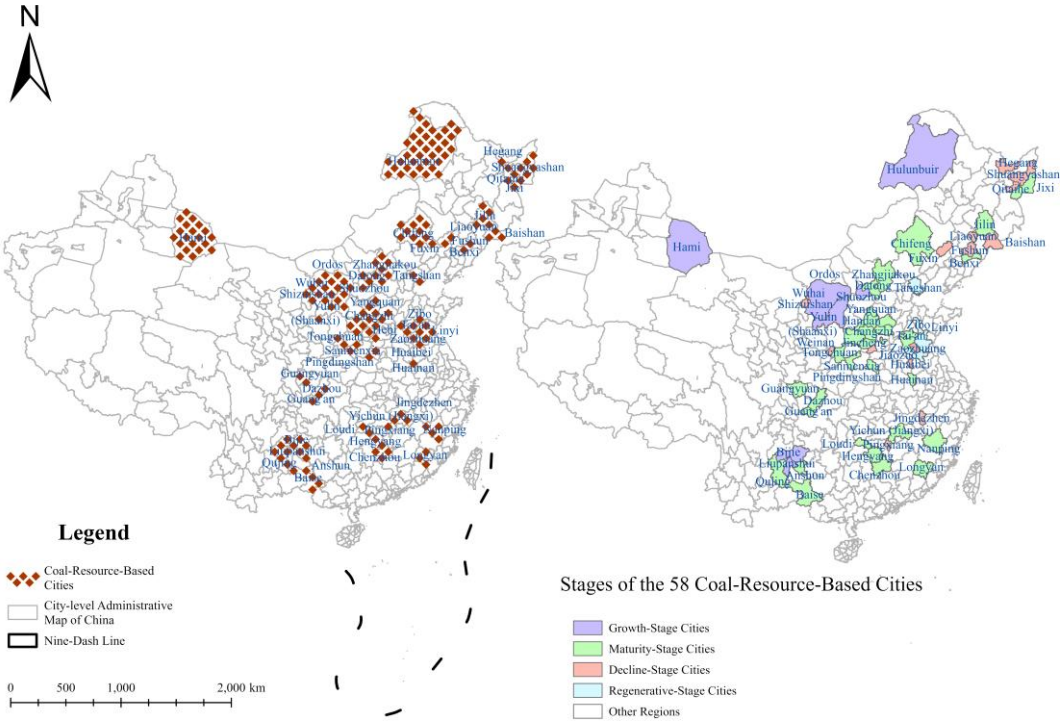

Figure 1. Spatial Distribution and Development Stages of China's Coal Cities

Coal-resource-based cities, serving as strategic anchors for national energy security, face a critical bottleneck in achieving the Dual Carbon Goals—constrained by the inherent contradiction between their high-carbon-emission characteristics and delayed decoupling progress. Systematically analyzing the spatiotemporal differentiation patterns of land-use carbon emissions and multi-scale driving mechanisms in such cities can contribute China's insights to global resource-based regions in exploring synergistic pathways for industrial transition, land restoration, and carbon neutrality. Based on the list of 262 resource-based cities defined in *China's Sustainable Development Plan for Resource-Based Cities (2013–2020)* and combined with the classification criteria for resource-based cities proposed by Jiang Dongmei et al. (Feng et al., 2023; Zhong et al., 2019; Xu et al., 2024; Zhang et al., 2024; Li et al., 2023), 58 typical coal-resource-based cities were selected through multi-source data matching and spatial overlay analysis. The spatial distribution of these cities exhibits a pattern of "abundance in the north and scarcity in the south, dense in the west and sparse in the east", which aligns closely with the macro-distribution characteristics of China's coal resource endowments (Figure 1). Figure 1 illustrates the developmental stages of the 58 coal-

resource-based cities (prefecture-level), categorized as follows: 7 growth-stage cities, 32 maturity-stage cities, 15 decline-stage cities, and 4 regenerative-stage cities.

2.1.2 Data Sources

Given the inconsistent statistical standards and systematic data gaps in pre-2000 socioeconomic data, coupled with the five-year interval updates and incomplete post-2020 land use datasets, this study confines its temporal scope to 2000–2020 to ensure data quality and comparability. Data collection encompasses four dimensions (Table 1): (1) Land use data: Derived from the China Land Cover Dataset (CLCD) with 30-meter resolution annual land use raster data (2000–2020) (Yang et al., 2021), calibrated using land use change survey data for resource-based cities published in China Statistical Yearbooks to establish spatiotemporally consistent time-series datasets; (2) Energy consumption data: Includes fossil fuel consumption (coal, petroleum, natural gas) sourced from city-level cross-sectional data in China Energy Statistical Yearbooks; (3) Socioeconomic data: Comprising population, GDP, and industrial structure indicators, integrated from China City Statistical Yearbooks, China Rural Statistical Yearbooks, and provincial statistical yearbooks; (4) Ecological data: Incorporating TEM, PRE, DEM terrain, and soil organic carbon density, with soil data extracted from China's Second National Soil Survey 1:1,000,000 vector database, and vegetation carbon sink coefficients matched using the 1:1,000,000 Vegetation Type Map of China.

A unified classification system was adopted to reclassify land use types into six categories: cropland, forestland, grassland, built-up land, water bodies, and unused land. A panel dataset for 294 Chinese prefecture-level cities (2000–2020) was constructed through multi-source data integration, with key technical processes including: (1) Missing data imputation: Combining linear interpolation, temporal moving average methods, and literature-based parameter ratios for data reconstruction; (2) Spatial allocation algorithm: Addressing missing city-level agricultural data via an arable land area proportion weighting method for spatial downscaling; (3) Spatial analysis: Calculating shortest Euclidean distances to provincial capitals and primary rivers, extracting DEM slope data using ArcGIS, and estimating regional vegetation carbon sink averages via spatial weighting.

2.1.3 Indicator System

The driving mechanisms of land use-related carbon emissions can be attributed to the combined effects of natural and socioeconomic factors (Huang et al., 2024; Li et al., 2023; Mu et al., 2023; Wei

et al., 2024; Hou et al., 2022; Yue et al., 2022; Zhu et al., 2023). By comprehensively considering data availability and representativeness principles for the study area, this study constructs an indicator system characterizing the driving factors of territorial spatial carbon effects in coal-resource-based cities (as shown in Table 1).

Tab.1 Indicator System for Driving Factors of Carbon Effects in National Space of Coal Resource-Based Cities

Category	Element	Indicator	Data Source	Description
Natural Factors	Topography	Slope (°)	Computer Network Information Center, CAS (www.gscloud.cn)	Topography is a key factor influencing land use/cover. Elevation and slope impose constraints on land development and utilization.
		Elevation (DEM, m)		
	Climate Influence	Temperature (TEM, °)	China Meteorological Data Service Center (http://data.cma.gov.cn)	Temperature and precipitation determine water and organic matter availability, thereby affecting land use-related carbon emissions.
		Precipitation (PRE,mm)		
	Location Factors	Distance to provincial capital (D-provincial capital, km)	National Geomatics Center of China (NGCC)	Location regulates land use type and intensity, thereby altering regional carbon emissions.
		Distance to primary rivers (D-River, km)		Rivers play a significant role in shaping regional landscapes, influencing land use-related carbon emissions.
Socioeconomic Factors	Demographic Factors	Total population (POP, Ten thousand people)	China City Statistical Yearbook and provincial statistical yearbooks	Population, industrial structure, and other socioeconomic factors dominate intensive land use [(Li et al., 2023)].
		Non-agricultural population (NAP, Ten thousand people)		
		Non-agricultural population ratio (NAPR, %)		
		Employment in mining industry (EMI, Ten thousand people)		
	Economic & Industrial Structure	Fixed asset investment (FAI, Ten thousand CNY)		
		GDP (Ten thousand CNY)		
		Energy Consumption (E-Consumption, Ten thousand CNY)		
		Proportion of secondary industry (PSI, %)		
		Proportion of tertiary industry (PTI, %)		
	Land Use	Proportion of cropland area (PCA, %)	China Land Cover Dataset (CLCD)	Urban land use types directly influence land use-related carbon emissions.
		Proportion of forest area (PFA, %)		Proportion of forest area
		Change rate of forest area (CRFA, %)		
		Proportion of water bodies (PWB, %)		
		Change rate of water bodies (CRWB, %)		
		Proportion of urban-industrial land (PUL, %)		
		Road network density (RND, %)		
	Science & Environmental Protection	Science and technology investment (STI, Ten thousand CNY)	China City Statistical Yearbook and provincial statistical yearbooks	Socioeconomic factors such as science/education investment and policies play dominant roles in intensive land use.
		Education investment (Edu-investment, Ten thousand CNY)		
		Comprehensive utilization rate of industrial solid waste (CURISW,%)		
		Harmless treatment rate of municipal solid waste (HTRMSW,%)		

2.2 Research Methodology

2.2.1 Calculation Methods for Land Use-Related Carbon Emissions

From dual perspectives of carbon sources and sinks, and building upon previous research, this study systematically quantifies carbon emissions across land use types by integrating the direct emission factor approach with indirect estimation methods, while accounting for the impacts of human economic activities. Given the complexity and spatial heterogeneity inherent in carbon cycle processes, the measurement necessitates the establishment of a standardized classification system and criteria, incorporating established carbon accounting frameworks within the field. The calculation formulas for carbon emissions by land use type are organized as follows:

(1) Carbon Emission Calculation for Cropland

Carbon emissions from cropland utilization primarily arise from agricultural input consumption, N_2O emissions during crop cultivation, CH_4 emissions from rice growth, as well as organic carbon mineralization and carbon uptake by crops (Zhou et al., 2021). Drawing on relevant literature, the net carbon emission effect of cropland utilization can be calculated as:

$$CE_{Arable} = CE_{FarmInputs} + CE_{N_2O} + CE_{CH_4} - CE_{OCM} - CA_{CropGrowth} \quad (1)$$

where CE_{Arable} denotes net carbon emissions from cropland; $CE_{FarmInputs}$、CE_{N_2O}、CE_{CH_4}、CE_{OCM}, and $CA_{CropGrowth}$ represent carbon emissions from agricultural inputs, N_2O emission conversion during crop cultivation, CH_4 emission conversion during rice growth, organic carbon mineralization, and carbon absorption by crop growth, respectively(Tian et al., 2013; Shao et al., 2014; Min et al., 2012; Chen et al., 2024).The carbon emissions from agricultural inputs are calculated as:

$$CE_{FarmInputs} = \sum I_i * E_i \quad (2)$$

where I_i and E_i denote the quantities of pesticides, fertilizers, agricultural film, diesel consumption, irrigation area, and their corresponding carbon emission coefficients. The formulas for CE_{N_2O}、CE_{CH_4}、CE_{OCM} and $CA_{CropGrowth}$ are:

$$\begin{cases} CE_{N_2O} = \sum PCrop_i * ECrop_{i_N_2O} \\ CE_{CH_4} = \sum PCrop * ECrop_{CH_4} \\ CE_{OCM} = E_{OCM} * A_{OCM} \\ CA_{CropGrowth} = \sum PCrop_i * ACrop_i \end{cases} \quad (3)$$

Where，$PCrop_i$ and $ECrop_{i_N_2O}$are the yield and N_2O emission conversion coefficient for the i-th crop type; $ECrop_{CH_4}$is the CH_4 emission conversion coefficient for rice; E_{OCM} and A_{OCM} represent soil organic carbon content and annual mineralization rate in cropland; $ACrop_i$is the

carbon sink coefficient for the i-th crop type.

(2) Carbon Emission Calculation for Urban-Industrial/Rural Residential Land

The net carbon emissions from urban-industrial and rural residential land are calculated based on energy consumption and population respiration within these areas. The formula is expressed as:

$$CE_{Ub_Rl} = CE_{Eng} + CE_{Pop} \quad (4)$$

Where， CE_{Ub_Rl} represents the net carbon emissions from urban-industrial/rural residential land; CE_{Eng} and CE_{Pop} denote carbon emissions from energy consumption and population respiration, respectively (Li et al., 202023; Kuang et al., 2010;Lai ., 2010; Zhao et al., 2013). The specific formulas for energy consumption and population-related emissions are:

$$\begin{cases} CE_{Eng} = \sum Cnsmp_{Eng_i} * E_{Eng_i} \\ CE_{Pop} = \sum P_{Pop} * E_{Pop} \end{cases} \quad (5)$$

Where， $Cnsmp_{Eng_i}$ and E_{Eng_i} are the consumption and carbon emission coefficient of the i-th energy type; P_{Pop} and E_{Pop} represent the population size and per capita respiration emission coefficient.

(3) Carbon Absorption Calculation for Forest Land

Forest land predominantly functions as carbon sinks. The carbon absorption capacity is calculated based on vegetation types and their corresponding carbon sink coefficients. The carbon effect formula for forest land is expressed as (Kuang et al., 2010):

$$CA_{Veg} = \sum Area_{Veg_i} * A_{Veg_i} \quad (6)$$

where: CA_{Veg} represents the carbon absorption of forest land; $Area_{Veg_i}$ denotes the area of the i-th vegetation type in forest land; A_{Veg_i} is the carbon sink coefficient for the i-th vegetation type.

(4) Carbon Absorption Calculation for Grassland, Water Bodies, and Unused Land

The carbon effects of grassland, water bodies, and unused land primarily manifest as carbon sink effects. These land types are calculated using the carbon sink coefficient method, with the formula defined as (Chen et al., 2024):

$$CA_{LU_i} = Area_{LU_i} * E_{LU_i} \quad (7)$$

Where， CA_{LU_i} denotes the carbon absorption of grassland, water bodies, or unused land; $Area_{LU_i}$ and E_{LU_i} represent the area and carbon sink coefficient of the i-th land use type, respectively.

2.2.2 Analytical Methods for Driving Forces of Land Use-Related Carbon Emissions

The driving mechanisms of land use-related carbon emissions were analyzed using a stepwise multiple regression model. This method effectively addresses multicollinearity issues through variance inflation factor (VIF) tests and stepwise variable selection, making it suitable for carbon flux attribution analysis under multivariate synergistic effects. In this study, urban land use-induced carbon emissions were designated as the dependent variable, while indicators of influencing factors for land use-related carbon emissions served as independent variables. This approach enables systematic analysis and identification of key factors affecting urban carbon emissions, thereby providing a scientific basis for urban land use planning and carbon reduction strategy formulation. A linear regression equation was constructed based on the collected dataset:

$$Y = \beta_0 + \beta_1 * + \beta_2 * X_2 + \cdots + \beta_n * X_n + \varepsilon \quad (8)$$

In the equation, Y represents the total carbon emissions from land use in each city, $(X_1, X_2, X_3 \cdots, X_n)$ denote the independent variables influencing land use-related carbon emissions, $(\beta_1, \beta_2, \beta_3 \cdots, \beta_n)$ are the regression coefficients for each influencing factor, and ε is the error term. The sign and magnitude of the regression coefficients reflect the direction and strength of each independent variable's impact on the dependent variable. Through this comprehensive assessment, a more holistic understanding of the complex relationship between urban land use and carbon emissions can be achieved.

The regression coefficients of driving factors for carbon emissions in each city were obtained via multiple linear regression analysis, followed by contribution degree evaluation. The contribution degree quantifies the relative importance of each indicator in influencing carbon emissions. This analysis not only reveals the explanatory strength of different drivers on emission variations but also elucidates the formation mechanisms underlying the spatial differentiation of these drivers. The relative contribution degree of each influencing factor is calculated as:

$$w_{ij} = \frac{|\beta_{ij}| \times \bar{X}_{ij}}{\sum_{i=1}^{m} \sum_{j=1}^{n} |\beta_{ij}| \times \bar{X}_{ij}} \quad (9)$$

where m=58, n=18, w_{ij} represents the contribution of driving factor j to carbon emissions in city i, $|\beta_{ij}|$ is the absolute value of the regression coefficient for factor j in city i, and $\bar{X}_{ij}$ denotes the mean value of the corresponding independent variable.

2.2.3 Analytical Methods for Spatiotemporal Differentiation of Land Use-Related Carbon Emissions

The center of gravity migration model is a method to determine the equilibrium position of a specific attribute at a given moment. By analyzing the spatial changes in the center of gravity of land use-related carbon emissions in coal-resource-based cities, this model further reveals the spatiotemporal evolution characteristics of territorial carbon emissions in these cities. The model typically involves the geometric coordinates of spatial objects and requires weighted processing based on their attribute values (Zhang et al., 2025； Dong et al., 2025). Through this approach, the weighted average attribute values of the objects can be calculated and comparatively analyzed to understand the characteristics of the target area, hence also referred to as the weighted average model (Wu et al., 2024).

$$X_i = \frac{\sum_{i=1}^{n} x_i * E_i}{\sum_{i=1}^{n} E_i}, \quad Y_i = \frac{\sum_{i=1}^{n} y_i * E_i}{\sum_{i=1}^{n} E_i}, \tag{10}$$

In the equation, X_i and Y_i represent the longitude and latitude of the carbon emission center of gravity, respectively; E_i denotes the carbon emissions from urban land use; x_i and y_i indicate the geographic coordinates of the cities.

Land use-related carbon emission hotspots refer to regions with significantly higher emissions, while coldspots denote areas with relatively lower emissions. Hotspot-coldspot analysis spatially identifies the clustering of high-value zones (hotspots) and low-value zones (coldspots) (Wu et al., 2024). The calculation formula is:

$$G^* = \frac{\sum_{i=1}^{n} Q_{ij} - \bar{a} \sum_{i=1}^{n} Q_{ij}}{\sqrt{\frac{\sum_{i=1}^{n} {a_i}^2}{n} - a^{-2}} \sqrt{\frac{\sum_{i=1}^{n} {Q_{ij}}^2 - \left(\sum_{i=1}^{n} Q_{ij}\right)^2}{n-1}}} \tag{11}$$

where G^* is the agglomeration index for grid a_i is the attribute value of grid *i*. Q_{ij} is the weight matrix, n is the total number of units, and $\bar{a}$ is the mean value of land use-related carbon emissions across all grids.

3. Result analysis

3.1 Land use carbon emission analysis

Coal-resource-based cities were categorized by their developmental stages, and trend diagrams illustrating the evolution of land use-related carbon emissions from 2000 to 2020 were generated accordingly. Figure 2 shows the changes in land use carbon emissions for growth-stage (7),

maturity-stage (32), decline-stage (15), and regenerative-stage (4) coal-resource-based cities. The figure clearly reveals that regenerative-stage cities exhibit significantly higher emission levels than other types, followed by growth-stage and maturity-stage cities, while decline-stage cities maintain the lowest emissions over time.

Growth-stage cities demonstrate a “stepwise growth-platform fluctuation” pattern in land use emissions, with most peaking post-2012. Their emission intensities show strong positive correlations with coal production expansion. Ordos and Yulin peaked above 25 million tons (Mt), while others generally peaked around 10 Mt. Notably, Hami and Yulin experienced secondary emission increases after short-term declines, reflecting carbon lock-in effects from energy infrastructure expansion during development. Other cities exhibited significant declines post-peak.

Among the 32 maturity-stage cities, 80% reached emission peaks below 25 Mt, yet inter-city variations were substantial, evident in both emission magnitudes and trends. Most peaked post-2010, with 22 cities showing significant declines afterward, while 4 displayed double-peak characteristics with 3–5-year lags relative to industrial upgrade cycles. Notably, Dazhou, Jining, Nanping, Yichun, and Changzhi exhibited continuous emission growth, driven by structural contradictions such as high reliance on resource-based industries, delayed emerging industry cultivation, and insufficient carbon sink development.

Decline-stage cities exhibited two key features: (1) overall low emission levels (peaks generally below 10 Mt) and (2) slower growth rates. Twelve cities achieved carbon peaking between 2008–2018 and entered sustained decline phases. However, Huaibei, Jingdezhen, and Pingxiang showed persistent increases, highlighting structural barriers during industrial transitions, particularly lagging energy efficiency improvements and slow clean energy adoption.

Regenerative-stage cities displayed notably higher emissions (peaks: 25–40 Mt) than other stages, attributed to dual factors: high-energy-consuming industrial agglomeration during resource regeneration and low efficiency in circular economic systems. Importantly, the carbon peaking timelines of regenerative-stage cities lagged significantly behind other types, reflecting delayed policy responses due to heavy industrial structures hindering low-carbon technology penetration.

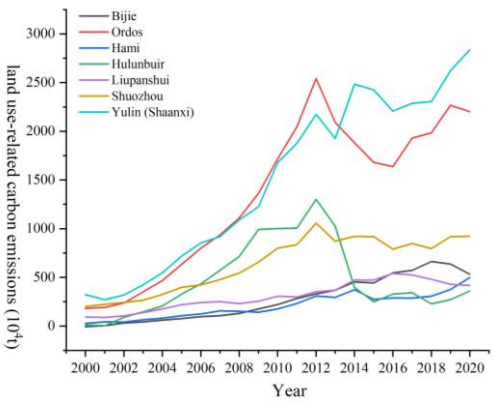

(a) Growth-stage cities

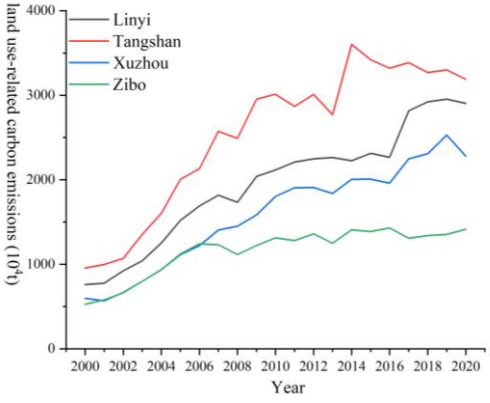

(b) Regenerative-stage cities

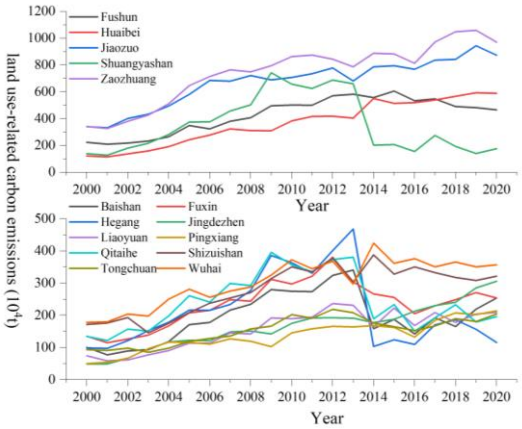

(c) Decline-stage cities

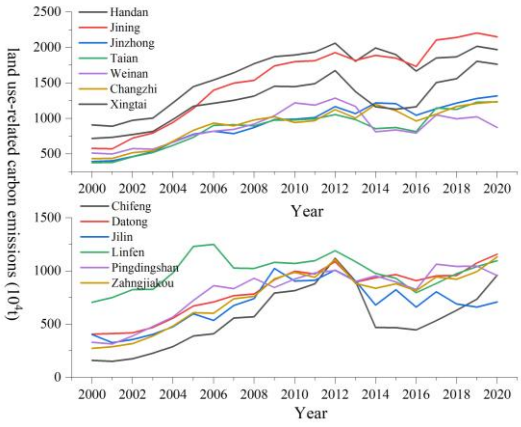

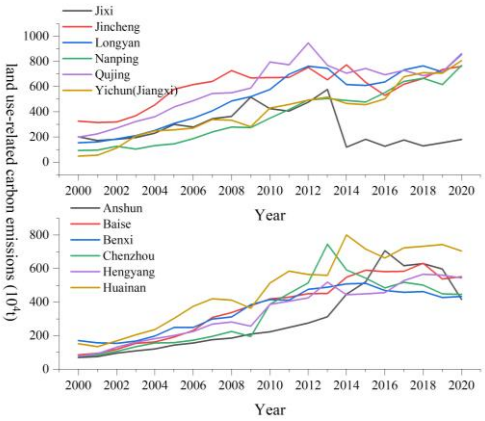

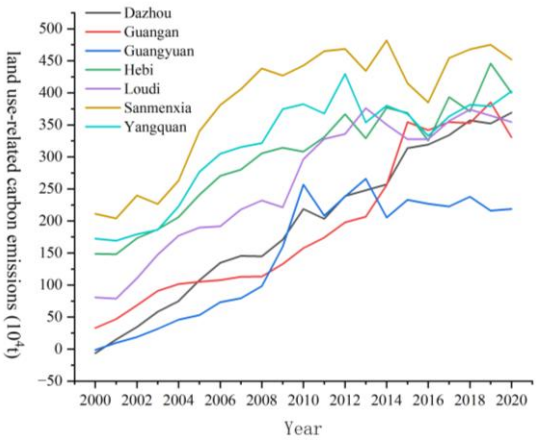

(d) Maturity-stage cities

Figure 2 Trends in land use-related carbon emissions of China's coal-resource-based cities from 2000 to 2020

3.2 Multiple Linear Regression Analysis

3.2.1 Initial Variable Screening

Based on panel data from 294 prefecture-level administrative units (including autonomous prefectures, regions, and provincial capitals) in China from 2000–2020, a global baseline model was first constructed to assess inter-variable association strengths prior to grouped regression modeling. Pearson correlation analysis (Table 2) revealed that over 70% of the selected driving factors passed significance tests at the 0.01 level, confirming their statistically significant associations with land use-related carbon emissions. Specifically, the driving factor coefficients exhibited notable heterogeneity: absolute correlation coefficients for POP, FAI, GDP, STI, Edu-investment, PUL, standard coal consumption, RND, and employment in the mining industry all exceeded 0.4. This indicates that these indicators exert significant positive impacts on land use-related carbon emissions—increases in these indicators promote regional carbon emissions. In contrast, negative correlation indicators exhibited smaller absolute coefficients compared to positive ones.

Based on a sample of 58 typical coal-resource-based cities, this study employed stepwise multiple linear regression modeling for variable screening. Initial regression analysis revealed that among 26 initial influencing factors, four variables—NAP, NAPR, GDP, and Edu-investment—exhibited variance inflation factor (VIF) values exceeding 10, indicating severe multicollinearity. These variables were removed following econometric principles. In the second-stage modeling, regression analysis showed that the VIF values for Slope and PFA still exceeded 5, suggesting moderate collinearity, leading to their further elimination (as shown in Figure 3).

Tab. 2: Pearson Correlation Coefficient Values between Carbon Emissions and Independent Variables

Factor	Correlation Coefficient	Factor	Correlation Coefficient
DEM	-0.238**	STI	0.483**
Slope	-0.355**	Edu-investment	0.648**
TEM	-0.035	PCA	0.243**
PRE	-0.178	PFA	-0.341**
D-Provincial Capital	-0.067**	CRFA	0.029
D-River	-0.059**	PWB	0.118**
POP	0.488**	CRWB	-0.068**
NAP	0.034	PUL	0.591**
NAPR	-0.02	RND	0.466**
FAI	0.535**	EMI	0.424**
GDP	0.812**	CURISW	-0.037
PSI	0.177**	HTRMSW	0.335**
PTI	0.039	E-Consumption	0.994**

** indicates significance at the 0.01 level (two-tailed), and * indicates significance at the 0.05 level (two-tailed).

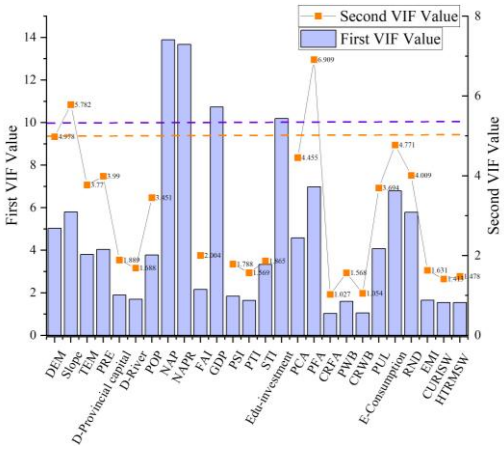

Fig. 3 Multicollinearity Test Results

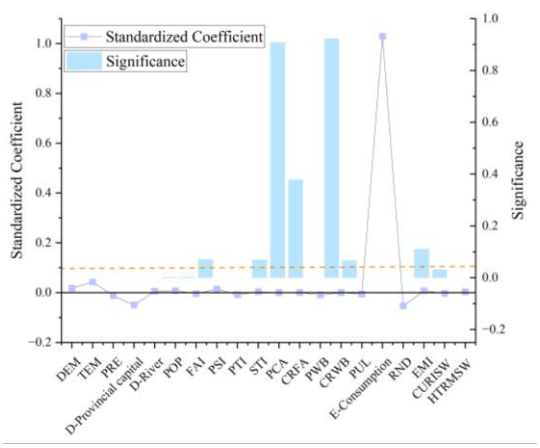

Fig. 4 Multiple Linear Regression Results

After two rounds of variable screening, the third regression analysis (Figure 4) demonstrated that the standardized regression coefficient for E-Consumption approached 1, significantly higher than other factors (all below 0.1). Given the direct linear transmission mechanism between E-Consumption and carbon emissions, this study isolated this variable in the driving force analysis module to avoid endogeneity bias in explanatory variables, adhering to econometric modeling standards for accurately analyzing indirect drivers such as industrial structure and technological advancement.

3.2.2 Stage-Specific Differences in Driving Factors of Carbon Emissions from Coal Cities

Based on multi-source datasets from 58 coal-resource-based cities in China, this study constructed grouped multiple linear regression models to reveal heterogeneity in carbon emission driving mechanisms across developmental stages. After systematic screening, the framework was established as follows: land use-related carbon emissions served as the dependent variable, with 18 core drivers (DEM, TEM, PRE) as independent variables. Cities were categorized into four groups—growth-stage (7), maturity-stage (32), decline-stage (15), and regenerative-stage (4)—for comparative modeling based on lifecycle theory. Empirical results (Figure 5) demonstrate significant spatial differentiation in emission driving mechanisms across stages:

Topographic-climatic factors exhibit stepwise attenuation patterns. DEM exerts the strongest driving effect in growth-stage cities (contribution: 0.256), significantly higher than in maturity-stage (0.094), decline-stage (0.056), and regenerative-stage cities (0.134). TEM shows inverse impacts, with contributions in maturity-stage (0.145) and decline-stage cities (0.201) being 3.3 times and 4.5 times higher than in growth-stage cities. These findings indicate a strong dependency on topographic selection during early development, where 25.6% of carbon emission variance in growth-stage cities is explained by elevation.

Location factors: The contribution of D-Provincial Capital in growth-stage (0.320) and regenerative-stage cities (0.164) is 1.8 times and 10.7 times higher than in maturity-stage (0.173) and decline-stage cities (0.030). Notably, the correlation between emissions and D-Provincial Capital in growth-stage cities far exceeds the influence of D-River (4.6%), highlighting the dominant regulatory role of provincial administrative resources during initial development.

Demographic-economic factors display lifecycle characteristics. The population agglomeration effect in regenerative-stage cities contributes 24.9% to emissions—2.4 times higher than in growth-stage cities (10.5%)—reflecting added emission pressures from population. In maturity-stage cities, employment in mining shows low contribution (0.039), revealing the inertia of existing labor forces in maintaining production patterns. Decline-stage cities exhibit dual lock-in effects from secondary industry proportion (0.079) and urban-industrial land use (0.162), where a 1% increase in secondary industry proportion raises emissions by 7.9%.

Land use factors: In decline-stage cities, the combined contribution of cropland proportion (0.111) and industrial-mining land (0.162) accounts for 27.3% of total driving forces, indicating constraints from delayed land function transitions on low-carbon transitions. Conversely, water

body area in maturity-stage cities offsets 12.9% of emission pressures through ecological regulation (contribution: 0.129).

Science-education-environmental factors show limited efficacy, with contributions from industrial solid waste utilization and waste treatment rates remaining below 3% across all groups. Notably, regenerative-stage cities exhibit a mere 0.5% contribution from environmental technologies, exposing structural mismatches between green innovation and developmental stages.

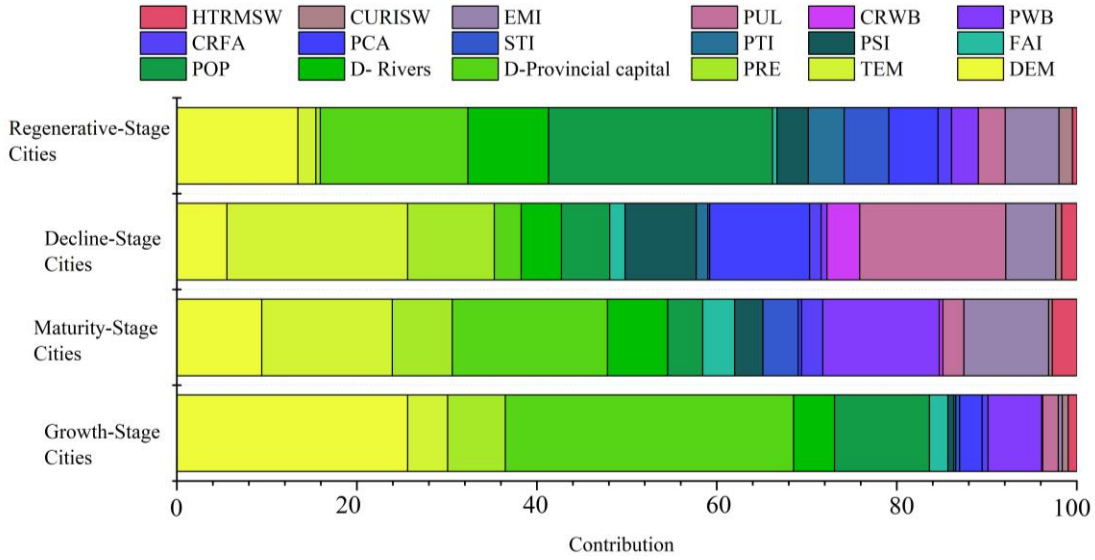

Fig. 5 Multivariate Linear Regression Results of Carbon Emission Impact Factors for Different Types of Cities' Land Use

In summary, the contribution of driving factors to land use-related carbon emissions exhibits significant heterogeneity across different functional types of cities. At the primary indicator level, topography and climatic conditions universally demonstrate substantial impacts on land use-related carbon emissions. Growth-stage coal-resource-based cities exhibit stronger dependencies on locational conditions, leading to higher carbon emissions during land use processes. Demographic factors, economic levels, and industrial structure exert relatively weaker influences, while technological and environmental protection factors show minimal impacts on land use-related carbon emissions.

3.2.3 Directionality Analysis of Key Driving Factors

To further compare the mechanisms of influencing factors across developmental stages of coal-resource-based cities, this study analyzed the directionality of factors with significant impacts (absolute contribution values > 0.1) in the four developmental stages. Figure 6 illustrates the directional effects of land use-related carbon emission drivers in coal-resource-based cities at different developmental stages.

The analysis reveals that for growth-stage cities, factors such as DEM, D-Provincial Capital, PRE, and PWB exhibit significant negative impacts on regional carbon emissions, whereas population and employment in the mining industry show strong positive impacts. Specifically: DEM and D-Provincial Capital suppress emissions by amplifying marginal infrastructure construction costs and reducing land development intensity due to topographic constraints, thereby limiting the agglomeration of energy-intensive industries. Increased geographical distance from provincial capitals weakens policy spillover effects and industrial gradient transfers, indirectly lowering emission intensity from extensive land use.

Conversely, population growth and expansion of mining industry employment drive emissions through two pathways: Urban population agglomeration directly stimulates spatial expansion of industrial and built-up land. Mining development elevates land demand for energy-intensive industries via industrial chain linkages. The synergistic effects of these factors result in significant increases in regional land use-related carbon emissions.

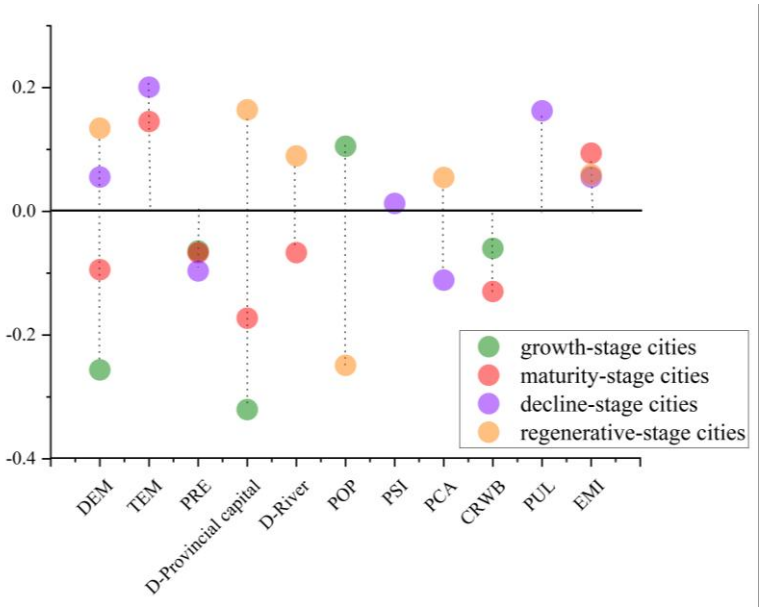

Fig. 6 The positivity/negativity of the impacts of key carbon emission factors in coal-resource-based cities

For maturity-stage coal-resource-based cities, DEM, PRE, D-Provincial Capital, D-River, and PWB act as negative influencing factors, while TEM and employment in the mining industry exhibit positive impacts. Similar to growth-stage cities, D-Provincial Capital remains significant, though the influence of DEM diminishes. Meanwhile, the ecological roles of PRE, rivers, and water bodies partially offset anthropogenic emissions. Notably, TEM—alongside mining employment—shows a pronounced positive impact, indicating reduced sensitivity to provincial capital spillover effects, weakened topographic constraints, and heightened temperature sensitivity as development progresses (land use emissions become more vulnerable to rising temperatures).

In decline-stage cities, DEM, TEM, PSI, PUL, and mining employment positively influence emissions, while PRE and cropland proportion act as negative factors. Compared to maturity-stage cities, emissions here are more strongly driven by secondary industry reliance and urban-industrial land use, reflecting deep-rooted dependencies on traditional energy systems. The carbon reduction effect of cropland is markedly higher than in other city types, underscoring the imperative for industrial restructuring amid resource depletion and the critical role of ecological restoration through land rehabilitation in emission mitigation. For regenerative-stage cities, DEM, D-Provincial Capital, D-River, and cropland proportion positively correlate with emissions, whereas population exerts a negative influence. During industrial transition, terrain-driven constraints elevate emissions via infrastructure layouts, while cities lacking locational advantages face declining high-tech industries and increased emissions from outdated industrial units. However, structural dividends from human capital-driven technological innovation and service-oriented consumption upgrades enable population factors to play a pivotal role in reducing land use-related emissions.

The heterogeneity of these driving factors directly shapes the spatial differentiation pattern of carbon emissions. To validate the spatial manifestation of this mechanism, this study further reveals its geographical distribution characteristics through hotspot analysis and gravity center migration.

3.3 Spatiotemporal Differentiation Analysis of Land Use-Related Carbon Emissions

The previous driving factor analysis revealed significant heterogeneity in carbon emission mechanisms across coal cities at different developmental stages. Such heterogeneity inevitably manifests in spatial patterns—regional agglomeration of high-contribution drivers will form emission hotspots, whereas areas dominated by inhibitory factors exhibit coldspot characteristics. To validate this hypothesis, this study employs hotspot analysis and gravity center migration to decipher the spatial differentiation of carbon emissions.

3.3.1 Hotspot-Coldspot Analysis for Coal-Resource-Based Cities

The spatial distribution characteristics of land use-related carbon emissions across 58 coal-resource-based cities were analyzed using the hotspot-coldspot method. As shown in Figure 7, from 2000 to 2020, the hotspot and coldspot patterns of land use-related carbon emissions in these cities underwent significant changes. In 2000, emission hotspots were concentrated in Liaoning, Hebei, Inner Mongolia, Shanxi, Henan, and Jiangsu provinces. Additionally, Jingdezhen City (Jiangxi) and

Nanping City (Fujian) were identified as hotspots. Coldspots were primarily distributed in Guizhou and Guangxi. By 2005, the hotspot areas decreased compared to 2000, with Jingdezhen and Nanping transitioning to non-significant regions. Coldspots expanded to include coal-resource-based cities in Heilongjiang Province, alongside Guizhou and Guangxi.

From 2000 to 2020, the areas of highly significant hotspots and significant hotspots substantially outnumbered coldspots, with the number and distribution of coldspots remaining relatively stable. This pattern reveals that coal-resource-based cities in densely clustered regions—such as Liaoning, Hebei, Inner Mongolia, Shanxi, Henan, and Jiangsu—exhibited higher land use-related carbon emissions. Concurrently, urbanization and industrialization processes in these regions exerted stronger impacts on urban land use patterns. In contrast, coal-resource-based cities in Yunnan, Guizhou, and Heilongjiang provinces demonstrated lower emissions, closely linked to the carbon sink effects of cropland and forestland. These natural carbon sinks played a critical role in reducing land use-related emissions, contributing to climate change mitigation.

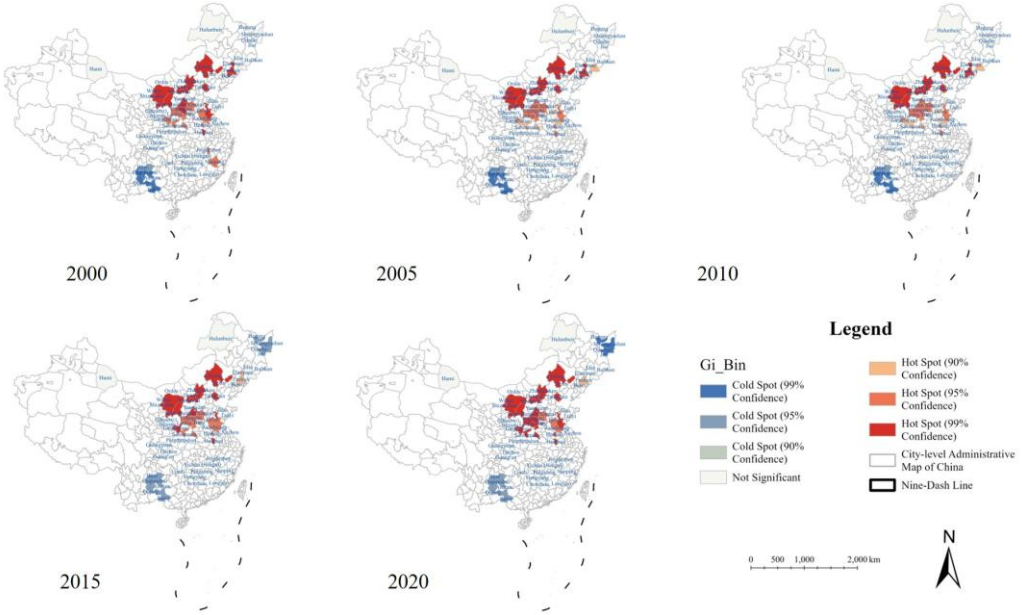

Fig. 7 Cold and Hot Spot Analysis Results of Land Use Carbon Emissions in Coal-Resource-Based Cities from 2000 to 2020

3.3.2 Analysis of the Migration of Carbon Emission Gravity Center of Land Use in Coal Resource-Based Cities

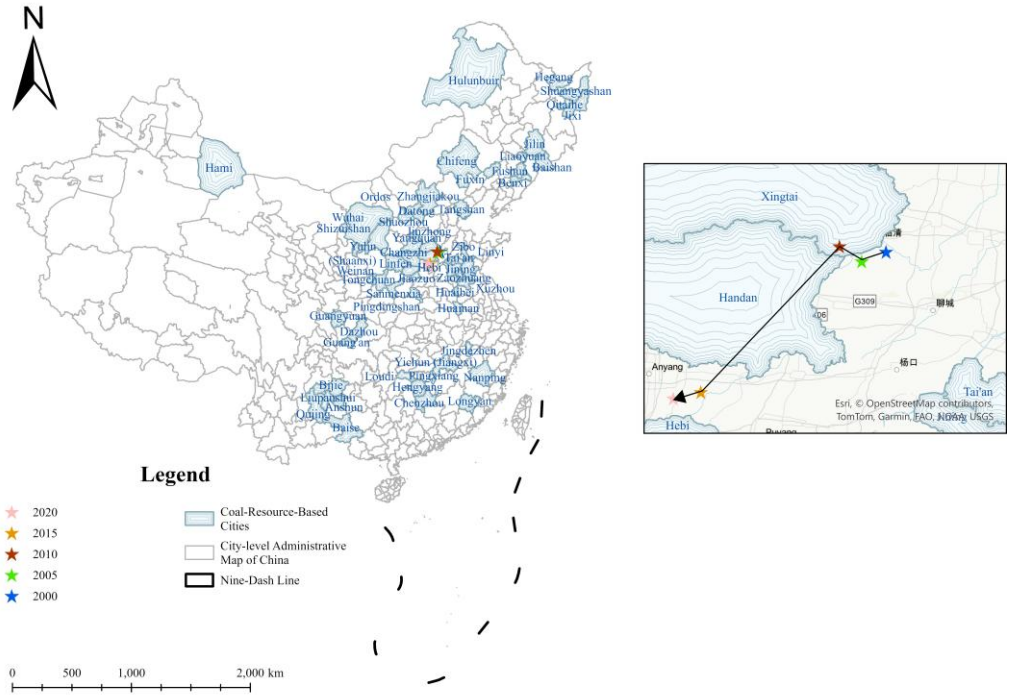

Figure 8 Average Centroid Shift of Carbon Emissions from Land Use in Coal Resource-based Cities

To reveal the spatiotemporal evolution characteristics of land use-related carbon emissions in coal-resource-based cities, the mean centers of gravity were calculated using five time-period datasets (2000, 2005, 2010, 2015, and 2020), with their migration trajectory visualized in Figure 8. The results indicate that the average center of land use-related carbon emissions for these cities was consistently located in Central China during 2000–2020. Specifically, the emission center exhibited an east-to-west and gradual southward migration: situated in Shandong Province in 2000, shifting to Hebei Province by 2010, and entering Henan Province after 2015. This trajectory aligns with the overall spatial distribution patterns of land use-related carbon emissions nationwide, while also reflecting the spatial characteristics of land use development in coal-resource-based cities.

Spatial differentiation patterns of carbon emissions reveal that: (1) The emission hotspots in regenerative cities, driven by population agglomeration and industrial land expansion, should spatially coincide with the energy-intensive industrial clusters in North China; (2) The carbon sink effect of water bodies in mature cities rich in water resources results in these cities exhibiting cold spot characteristics; (3) The post-2015 southward shift of the gravity center to Henan Province aligns with the expansion of southern coldspots caused by the negative contribution of cropland proportion in decline-stage cities.

4 Conclusions

This study systematically reveals the spatiotemporal evolution patterns and driving mechanisms of carbon emissions in coal-resource-based cities based on China's prefecture-level land use carbon emission accounting framework. Key findings are as follows:

(1) Temporal Evolution Characteristics

During 2008–2018, most coal-resource-based cities sequentially reached peak land use-related carbon emissions and subsequently entered decline phases, while a minority exhibited continuous increases. Peaking timelines varied significantly across lifecycle stages: regenerative-stage cities peaked later than other developmental stages, with emission intensities following a hierarchy of regenerative-stage > growth-stage > maturity-stage > decline-stage, confirming the coupling between resource exploitation intensity and urban development stages.

(2) Driving Mechanisms

Growth-stage cities: Emissions are constrained by topographic and administrative locational factors. Maturity-stage cities: Emissions arise from interactions between thermal regulation (TEM) and production system inertia (mining employment). Decline-stage cities: Emissions are dominated by industrial structure (secondary industry proportion) and land use patterns (cropland proportion). Regenerative-stage cities: Emissions are mitigated by human capital (population quality).This pattern reflects a transition in emission mechanisms: from topographic constraints to industrial structure regulation, and ultimately to innovation-driven transformation.

(3) Spatial Differentiation Characteristics

From 2000 to 2020, land use-related carbon emissions in China's coal-resource-based cities exhibited an east-to-west and gradual southward trajectory, closely tied to spatial land use distribution. Hotspots migrated from Liaoning and Hebei toward central China (Henan), aligning with national emission distribution trends. Conversely, emissions remained lower in Yunnan, Guizhou, and Heilongjiang provinces.

5 Discussion

This study advances existing research through three key innovations: (1) establishing a scientific classification system for coal-resource-based cities grounded in developmental stage theory; (2) developing a unified accounting framework for land-use carbon emissions that systematically elucidates spatiotemporal evolution patterns during 2000–2020; and (3) precisely identifying stage-specific driving mechanisms to inform targeted carbon reduction policies.

Results demonstrate significant heterogeneity in driving mechanisms of land use-related carbon emissions across coal-resource-based cities at different stages. Topographic-climatic and locational factors serve as foundational drivers, but their intensity and directionality vary by developmental stage: Growth-stage cities exhibit high sensitivity to topographic elevation and D-Provincial Capital, indicating infrastructure development and policy spillover effects dominate early-stage emission patterns. Maturity-stage cities are positively driven by rising temperatures and mining industry expansion, with emerging ecological regulation from hydrological conditions. Decline-stage cities show strong positive impacts from secondary industry proportion and urban-industrial land use, highlighting emission reduction potential through industrial restructuring and land rehabilitation. Notably, regenerative-stage cities achieve emission suppression through human capital improvement and service sector development, but exhibit significantly delayed peaking times compared to other city types, which may be attributed to three key factors: carbon lock-in effects from legacy infrastructure, transitional frictions during industrial restructuring, and locational disadvantages hindering low-carbon technology diffusion (Huang et al., 2024). Furthermore, cropland area demonstrates significant carbon sink effects in decline-stage cities, whereas the mitigation contributions from technological and environmental factors remain relatively limited, underscoring the need to enhance the marginal benefits of technical mitigation measures.

The carbon governance of coal-resource-based cities requires establishing a dynamic, stage-adaptive policy system that implements differentiated strategies according to the characteristics of cities at different development stages. Specifically, growth-stage cities should optimize three-dimensional spatial planning to overcome topographic constraints while establishing low-carbon policy pilot zones. Maturity-stage cities need to develop a dual-drive mechanism combining climate resilience enhancement with green industrial upgrading. Decline-stage cities must integrate land ecological restoration with industrial restructuring to implement mandatory emission reduction measures. Regenerative-stage cities should focus on cultivating human capital and innovation ecosystems to accelerate low-carbon transition. It should be noted that current research still has limitations, including less precise carbon emission measurements due to data availability constraints and insufficient exploration of operational planning measures for different city types (Jia et al., 2023; Wu et al., 2025). Future studies should further refine carbon accounting methods and explore more actionable policy implementation pathways based on urban development contexts.

6 . Statements

6.1 Ethics approval

Consent.

6.2 Consent to participate

Agree to participate.

6.3 Consent for publication

Agreement for publication.

6.4 Funding

Not applicable.

6.5 Competing Interests

The authors have no relevant financial or non-financial interests to disclose.

6.6 Author Contributions

Chen Longgao supervised the research and proposed the research direction. Pan Yisha and Yang Xiaoyan were responsible for report analysis and paper writing. Liu Liangchen and Wang Chongyang responsible for data processing.

6.7 Data Availability

The datasets generated during and analyzed during the current study are available from the corresponding author on reasonable request.

References

Bao K Y, Ruan J, Zhu Y N, et al. (2023). Analysis on the resource and environmental carrying capacity of coal city based on improved system dynamics model: a case study of Huainan, China. Environmental Science and Pollution Research, 30: 36728-36743.

Calvillo C F, Katris A, Zhou L, et al. (2025). Jobs, skills and regional implications of the low carbon residential heat transition in the UK. Energy Policy, 202: 114579.

Cao J H, Xie C, Zhou Y, et al. (2025). Forecasting carbon price: A novel multi-factor spatial-temporal GNN framework integrating Graph WaveNet and self-attention mechanism. Energy Economics,

144: 108318.

Chen H, Qi S Z, Tan X J. (2022). Decomposition and prediction of China's carbon emission intensity towards carbon neutrality: From perspectives of national, regional and sectoral level. Science of The Total Environment, 825.

Chen L G, Wang X Y, Yang X Y, et al. (2024). Spatial and temporal differentiation of carbon effects and driving forces of cropland change: A case study of Jiangsu Province. Resources and Environment in the Yangtze Basin, 33(9): 1953-1968.

Dong H, Zhang P, Dong H B, et al. (2025). The spatiotemporal dynamic evolution characteristics of carbon emissions in less developed resource-based cities: evidence from Pingliang City, China. Scientific Reports, 15(1): 11266.

Feng Y L, Yan L H, Hao D D, et al. (2023). Effects of decadal nitrogen and phosphorus fertilization on microbial taxonomic and functional attributes associated with soil organic carbon decomposition and concentration in an alpine meadow. Ecological Indicators, 146.

Guan J, Peng Y. (2021). Does coal mining have effects on land use changes in a coal resource-based city? Evidence from Huaibei city on the north China plain. International Journal of Environmental Research and Public Health, 18(21).

Guan Y, Shan Y, Huang Q, et al. (2021). Assessment to China's recent emission pattern shifts. Earth's Future, 9(11).

Guevara M, Petetin H, Jorba O, et al. (2022). European primary emissions of criteria pollutants and greenhouse gases in 2020 modulated by the COVID-19 pandemic disruptions. Earth System Science Data, 14(6): 2521-2552.

Gu Q Y. (2023). Conceptual adjustment and dilemma resolution of China's territorial space governance under the dual carbon goals. China Land Science, 37(10): 12-19.

He Z H, Gu X L, Wang M Q, et al. (2025). The coupled effect of climate change and LUCC on meteorological drought in a karst drainage basin, Southwest China. Scientific Reports, 15(1): 9134.

Hou M Y, Deng Y J, Yao S B. (2022). Urbanization, intensive use of cultivated land and grain production: The regulated mediating effect under climatic conditions. China Population, Resources and Environment, 32(10): 160-171.

Hu J, Zheng C, Xu J, et al. (2024). The influence of supplier financial violations on clients' environmental, social, and governance performance: Evidence from China's manufacturing industry. Corporate

Social Responsibility and Environmental Management, 31(6): 6217-6233.

Huang H Z. (2024). Spatio-temporal pattern evolution of land use carbon emissions, influencing factors and carbon balance zoning in counties of Jiangxi Province. Jiangxi Normal University.

Huang H Z, Jia J S, Chen D L, et al. (2024). Evolution of spatial network structure for land-use carbon emissions and carbon balance zoning in Jiangxi Province: A social network analysis perspective. Ecological Indicators, 158 :111508.

Jia J S, Xin L L, Lu C F, Wu B, et al. (2023). China's CO_2 emissions: A systematical decomposition concurrently from multi-sectors and multi-stages since 1980 by an extended logarithmic mean divisia index. Energy Strategy Reviews, 49:101141.

Kuang Y Q, Ouyang T P, Zou Y, et al. (2010). Assessment of current carbon sources and sinks and potential for increasing carbon sinks in Guangdong Province. China Population, Resources and Environment, 20(12): 56-61.

Lai L. (2010). Study on the carbon emission effects of land use in China. Nanjing University.

Li X H, Liu Y S, Guo Y Z. (2023). The spatial pattern of population-land-industry coupling coordinated development and its influencing factor detection in rural China. Journal of Geographical Sciences, 33(11): 2257-2277.

Li Z J, Xu J L, Wang J, et al. (2023). Spatio-temporal heterogeneity of urban carbon emissions and influencing factors in the Yangtze River Economic Belt. Resources and Environment in the Yangtze Basin, 32(3): 525-536.

Liu Z, Guan D, Wei W, et al. (2015). Reduced carbon emission estimates from fossil fuel combustion and cement production in China. Nature, 524(7565): 335-338.

Min J S, Hu H. (2012). Estimation of greenhouse gas emissions from agricultural production in China. China Population, Resources and Environment, 22(7): 21-27.

Mi Z F, Zheng J L, Meng J, et al. (2019). Carbon emissions of cities from a consumption-based perspective. Applied Energy, 235: 509-518.

Mu J Y, Wang J M, Liu B, et al. (2023). Research progress on the evolution and influencing factors of carbon emissions in resource-based cities. Journal of China Coal Society: 1-15.

Renna P. (2024). Performance Evaluation of Reconfiguration Policy in Reconfigurable Manufacturing Systems including Multi-Spindle Machines: An Assessment by Simulation. Applied Sciences, 14(7).

Shao X F. (2014). Carbon and nitrogen accumulation and mineralization characteristics of black soil

aggregates under long-term organic fertilization. Wuhan University of Technology.

Tao B Y, Wu F P, Wang J G, et al. (2025). County-level source-sink balance and carbon allocation of regional peak emissions: Model construction and application. Ecological Indicators, 173: 113387.

Tian Y, Zhang J B. (2013). Spatial and temporal differentiation of net carbon effects in China's agricultural production. Journal of Natural Resources, 28(8): 1298-1309.

Wei J C, Mei Z X, Ma J J, et al. (2024). Spatio-temporal evolution of land use carbon emissions and influencing factors in Guangzhou City. Research of Soil and Water Conservation, 31(4): 298-307.

Wu H Y, Qiu Y G, Li Y, et al. (2022). Effects of China's land-intensive use on carbon emission reduction: A new perspective of industrial structure upgrading. Frontiers in Environmental Science, 10.

Wu X, Zhong S, Chen G, et al. (2025). Influence of land use intensity on urban carbon efficiency under a carbon neutrality target: Evidence from the Yangtze River Delta urban agglomeration, China. Environmental Impact Assessment Review, 110: 107689.

Wu Y G, Pu W P, Dong J H. (2024). Land use centroid changes and carbon accounting scenario simulation in the Chengdu Plain. Bulletin of Soil and Water Conservation, 44(5): 392-408.

Xu L F, Chen W L, Zhu H M, et al. Analysis of carbon emission characteristics and influencing factors of different land use types in Hunan Province. Environmental Science.

Yang J, Huang X. (2021). The 30 m annual land cover dataset and its dynamics in China From 1990 to 2019. Earth System Science Data, 13: 3907-3925.

Yue M T. (2022). Spatio-temporal pattern of spatial correlation network of urban carbon emission efficiency and influencing factors in China. East China Normal University.

Zeng S B, Zhang Y X, Jin G. (2025). Can urban low-carbon transformation affect the prices of its industrial land? An empirical study based on spatial regression discontinuity. Land Use Policy, 148: 107413.

Zhang L J, Yi J H, Yang S, et al. (2025). Analysis of non-uniform spatiotemporal evolution characteristics in Dongting Lake and Hong Lake using Sentinel-1A/B data from 2015 to 2022. Remote Sensing Letters, 16(4): 412-421.

Zhang L Z, Shi Y. (2025). A dynamic multi-objective optimization model for inner-industry carbon responsibility allocation based on carbon tax and carbon offsets accounting. Applied Energy, 377: 124571.

Zhang P Y, He J J, Hong X, et al. (2018). Carbon sources/sinks analysis of land use changes in China

based on data envelopment analysis. Journal of Cleaner Production, 204: 702-711.

Zhang X S, Nie D W, Chen Z Z, et al. Spatio-temporal evolution characteristics and influencing factors of carbon emissions in the construction industry in western China. Environmental Science.

Zhao R Q, Huang X J, Zhong T Y, et al. (2013). Carbon effect assessment and low-carbon optimization of regional land use structure. Transactions of the Chinese Society of Agricultural Engineering, 29(17): 220-229.

Zhou S Y, Xi F M, Yin Y, et al. (2021). Carbon emission accounting and driving factors of cultivated land utilization in Northeast China. Journal of Applied Ecology, 32(11): 3865-3871.

Zhu M, Gong W G. (2023). The impact of agricultural labor outflow on cultivated land abandonment and its formation mechanism. Economist, (9): 119-128.

Zhu Y K, Xia X S, Canadell J G, et al. (2025). China's carbon sinks from land-use change underestimated.